Simulations of non-neutral slab systems with long-range electrostatic interactions in two-dimensional periodic boundary conditions

V. Ballenegger,[1,a)] A. Arnold,[2] and J. J. Cerdà[3]
[1]*Institut UTINAM, Université de Franche-Comté, UMR 6213, 16 route de Gray, 25030 Besançon Cedex, France*
[2]*Fraunhofer Institute SCAI, Schloss Birlinghoven, 53754 Sankt Augustin, Germany*
[3]*Institute for Computational Physics, Universität Stuttgart, 70569 Stuttgart, Germany*

(Received 11 June 2009; accepted 12 August 2009; published online 3 September 2009)

We introduce a regularization procedure to define electrostatic energies and forces in a slab system of thickness h that is periodic in two dimensions and carries a net charge. The regularization corresponds to a neutralization of the system by two charged walls and can be viewed as the extension to the two-dimensional (2D)+h geometry of the neutralization by a homogeneous background in the standard three-dimensional Ewald method. The energies and forces can be computed efficiently by using advanced methods for systems with 2D periodicity, such as MMM2D or P3M/ELC, or by introducing a simple background-charge correction to the Yeh–Berkowitz approach of slab systems. The results are checked against direct lattice sum calculations on simple systems. We show, in particular, that the Madelung energy of a 2D square charge lattice in a uniform compensating background is correctly reproduced to high accuracy. A molecular dynamics simulation of a sodium ion close to an air/water interface is performed to demonstrate that the method does indeed provide consistent long-range electrostatics. The mean force on the ion reduces at large distances to the image-charge interaction predicted by macroscopic electrostatics. This result is used to determine precisely the position of the macroscopic dielectric interface with respect to the true molecular surface. © *2009 American Institute of Physics*. [doi:10.1063/1.3216473]

I. INTRODUCTION

The high interest in simulating surface and interfacial problems has led to an active search for efficient methods to compute long-range interactions in two-dimensional (2D) periodic systems that have a finite thickness (2D+h geometry). 2D Ewald-type formulas were derived by a number of workers.[1–6] As most of these methods scale quadratically with the number N of particles, other faster methods were proposed. The MMM2D method has an adjustable preset accuracy and scales as $N^{5/3}$,[7] see also Ref. 8. An approach with an almost linear scaling was proposed by Yeh and Berkowitz: It consists in introducing a gap in the simulation box along the nonperiodic dimension and to use a standard Ewald code for three-dimensional (3D) periodic systems with the summation order changed to slabwise (EW3DC method).[9] That method is accurate only when the gap in the simulation box is large enough. The errors introduced by the unwanted interactions with the layers artificially replicated in the nonperiodic direction can be exactly compensated for by adding an electrostatic layer correction (ELC) term, whose computational cost is linear in the number of particles. When that term is used in conjunction with a fast particle-mesh implementation of the Ewald sum, such as the P3M (Ref. 10) or SPME (Ref. 11) algorithm, the resulting methods P3M/ELC and SPME/ELC scale as $N\log(N)$. In the case of the P3M/ELC method, an error estimate is moreover available;[12] it allows the method to be tuned automatically to its optimal operation point, which minimizes the computational time at the desired accuracy. Another slab method with a $N\log(N)$ scaling was proposed recently by Ghasemi *et al.*[13] The distribution of errors is uniform across the slab in that latter method, contrary to P3M/ELC, but it has no *a priori* error estimate.

In all the aforementioned works, the system is assumed to be overall charge neutral. In some situations, for example, when studying surfaces with charged defects or when computing ionic solvation free energies near an interface, one needs a method applicable to a slab system carrying a net charge. The purpose of this paper is to define a regularization of the (divergent) lattice sum for the energy and to have an efficient way to compute the regularized energies and forces. This allows, for example, Monte Carlo and molecular dynamics simulations of non-neutral slab systems to be performed with long-range electrostatic interactions that are fully consistent with the 2D periodic boundary conditions (2D-PBC).

The regularization of the lattice sum via a suitable neutralization of the simulation cell is presented in Sec. II. The practical computation of these regularized sums is discussed in Sec. III for three recent efficient algorithms: EW3DC, P3M/ELC, and MMM2D. Numerical tests performed in Sec. IV show that the three methods give consistent results for energies and forces that agree as well with direct lattice sum calculations. In Sec. V, a molecular dynamics simulation of a sodium ion close to an air/water interface is performed to demonstrate that the method does indeed provide consistent long-range electrostatics.

[a)]Electronic mail: vincent.ballenegger@univ-fcomte.fr.

II. CHARGED SLAB IN 2D PERIODIC BOUNDARY CONDITIONS

A. Definition of energy and forces

We consider a slab system composed of N particles with charges q_i and positions $\boldsymbol{r}_i=(x_i,y_i,z_i)$ $(i=1,\ldots,N)$ in a simulation cell which is periodically replicated in the x and y directions with period L_x and L_y, respectively. In the nonperiodic z-direction, the system has a finite extent h, which can be arbitrarily large. Particle positions lie in the region delimited by $-L_x/2<x\leq L_x/2$, $-L_y/2<y\leq L_y/2$, and $-h/2\leq z\leq h/2$. The regions outside the slab, $z>h/2$ and $z<-h/2$, are assumed to be void; their dielectric permittivity is that of vacuum. The Coulomb energy in Gaussian units is given by the sum over periodic images,

$$E=\frac{1}{2}\sum_{n_x,n_y\in\mathbb{Z}}\sum_{i,j=1}^{N}{}'\frac{q_iq_j}{|\boldsymbol{r}_i-\boldsymbol{r}_j+n_x\boldsymbol{L}_x+n_y\boldsymbol{L}_y|}, \tag{1}$$

where $\boldsymbol{L}_x=L_x\hat{\boldsymbol{e}}_x$, $\boldsymbol{L}_y=L_y\hat{\boldsymbol{e}}_y$, and the prime denotes the omission of the $i=j$ term in the primary cell $n_x=n_y=0$. Notice that interactions between charges in the primary cell are accounted for with a factor 1, since they appear twice in the sum (1), while interactions of charges in the primary cell with charges in image cells $(n_x,n_y)\neq(0,0)$ are accounted for with a factor 1/2 since they appear only once in the sum. That factor 1/2 is necessary to avoid double counting in the energy of the simulated macroscopic sample, as explained in Appendix A.

The sum (1) is only defined for a charge neutral system $(\Sigma_i q_i=0)$, and even then, the sum is only conditionally convergent. This means that we need to specify the order in which we perform the sum. We adopt here the cylindrical limit, i.e.,

$$E=\lim_{R\to\infty}E(R), \tag{2}$$

with

$$E(R)=\frac{1}{2}\sum_{\substack{n_x,n_y\in\mathbb{Z}\\(n_xL_x)^2+(n_yL_y)^2\leq R^2}}\sum_{i,j=1}^{N}{}'\frac{q_iq_j}{|\boldsymbol{r}_i-\boldsymbol{r}_j+n_x\boldsymbol{L}_x+n_y\boldsymbol{L}_y|}. \tag{3}$$

Notice that the energy does not depend in the limit $R\to\infty$ on the dielectric constant ϵ' of the external medium in region $x^2+y^2>R^2$, contrary to the usual Ewald method for 3D-periodic systems, where the dielectric constant of the outer spherical medium at $x^2+y^2+z^2>R^2$ does intervene. The reason for this can easily be understood on physical grounds. Indeed, when the simulation cell is polarized, macroscopic electrostatics tells us that surface charges appear at the dielectric discontinuity between the external medium and the macroscopic sample made up of copies of the central simulation cell. The magnitude of these polarization surface charges depend on ϵ' and may produce a depolarizing field in the sample that contributes to the energy. In the case of a slab system, the charges induced on the side surfaces at $x^2+y^2=R^2$ are proportional to the area $2\pi Rh$, while the electric field created by them in the sample decays as R^{-2}. In the limit $R\to\infty$, that field vanishes, so that the energy is indeed independent of ϵ'. The energy of a slab system depends, however, on the dielectric permittivities ϵ_1 and ϵ_2 of the two regions above $(z>h/2)$ and below $(z<-h/2)$ the slab, which are here assumed to be empty $(\epsilon_1=\epsilon_2=1)$.

If some charges (electrons, counterions, etc.) are treated implicitly in the system, the total charge

$$Q_{\mathrm{tot}}=\sum_{i=1}^{N}q_i \tag{4}$$

of the simulation box can differ from zero. The energy (1) remains finite only if the background charge provided by the implicit particles is properly accounted for.

In systems with 3D periodicity where the implicit charges are assumed to provide a homogeneous and isotropic charge distribution, the background charge reduces to a uniform charge density $\rho_b=-Q_{\mathrm{tot}}/V$, where V is the volume of the simulation box. The standard Ewald method can be used to sum the Coulomb interactions in such systems, including the interaction with the neutralizing background, see e.g., Refs. 14 and 15. The Ewald formula for the energy of the 3D-periodic system takes then the form $E_{3\mathrm{D}}=E^{(r)}+E^{(k)}+E^{(d)}+E^{(n)}$, where the three first terms are the usual real-space, reciprocal-space, and surface contributions, while the last term is an electroneutrality contribution

$$E^{(n)}=-\frac{\pi Q_{\mathrm{tot}}^2}{2\alpha^2V} \tag{5}$$

that depends on the Ewald splitting parameter α. The energy $E_{3\mathrm{D}}$ is independent of the free Ewald parameter α only if the contribution $E^{(n)}$ is included. As the neutralizing background is homogeneous, the energy $E^{(n)}$ is independent of the particle positions and does thus not lead to any force.

For future reference, it is useful to recall the origin and physical content of term $E^{(n)}$. It corresponds merely to the sum of the direct-space interaction $E_{c\text{-}b}^{(r)}$ of the charged particles with the neutralizing background, and to the direct-space background-background interactions $E_{b\text{-}b}^{(r)}$ on the other hand. Thus $E^{(n)}=E_{c\text{-}b}^{(r)}+E_{b\text{-}b}^{(r)}$, where

$$E_{c\text{-}b}^{(r)}=\sum_i q_i\int_{\mathbb{R}^3}\psi(r)\rho_b d^3\boldsymbol{r}=-\frac{\pi Q_{\mathrm{tot}}^2}{\alpha^2V} \tag{6}$$

[see, e.g., Eq. (3.5) of Ref. 16] and

$$\begin{aligned}E_{b\text{-}b}^{(r)}&=\frac{1}{2}\int_V d\boldsymbol{r}\int_{\mathbb{R}^3}d\boldsymbol{r}'\,\rho_b\psi(|\boldsymbol{r}-\boldsymbol{r}'|)\rho_b\\&=\frac{\rho_b^2}{2}\int_V d\boldsymbol{r}\frac{\pi}{\alpha^2}\\&=\frac{\pi Q_{\mathrm{tot}}^2}{2\alpha^2V},\end{aligned} \tag{7}$$

where $\psi(r)=\mathrm{erfc}(\alpha r)/r$ is the direct-space interaction. Notice the factor 1/2 in the background-background energy that is needed to avoid double counting (see Appendix A). The reciprocal-space interaction of the particles with the background and the reciprocal-space background-background energy exactly cancel the corresponding singularity in the

charge-charge interactions. In the Ewald formula for a non-neutral system, they are included in the canceling of the (otherwise divergent) $\boldsymbol{k}=\mathbf{0}$ term in the reciprocal sum.

In a system with 2D periodicity, the background charge associated with the implicit particles can take different forms. For example, if these particles are homogeneously distributed in some confined region $[z_1,z_2]$ along the nonperiodic direction, they may be replaced by a uniform neutralizing slab in that region. That charged background slab will clearly give rise an inhomogeneous electric potential $V_0(z)$ and to forces on charged particles. If the implicit particles are not confined to some particular region of space, it is appropriate to introduce a neutralization of the simulation cell that does not introduce any background force on the particles. Having a neutralization with this property is especially useful because it is generic; it can be used to simulate systems with any other neutralizing background by simply adding the corresponding background electric potential $V_0(z)$ as an external field in the simulation.

Unlike the 3D case, a neutralization that does not exert forces cannot be realized in 2D-PBC by adding a uniform charge distribution over all space; therefore a different route is needed to deal with 2D systems with a net charge. We propose to simply substract the singularity that arises due to the excess charge, which can be calculated analytically as follows. The asymptotically diverging behavior of $E(R)$ as $R\to\infty$ can be found by approximating the slab as a charged sheet carrying a surface charge density $\sigma_{\text{sheet}}=Q_{\text{tot}}/(L_xL_y)$ and by noting that the divergence arises from the large distance contributions to the interaction energy of the simulation cell with this sheet. This divergence is

$$\frac{1}{2}Q_{\text{tot}}\int_0^R \frac{\sigma_{\text{sheet}}}{r}2\pi r dr = \frac{\pi Q_{\text{tot}}^2}{L_xL_y}R, \tag{8}$$

where the factor 1/2 ensures, as in Eq. (1), that one measures only half of the interaction energy of the simulation cell with the periodic copies of the cell (see Appendix A). Subtracting Eq. (8) from Eq. (3), we define the energy of a charged system in 2D-PBC as

$$E=\lim_{R\to\infty}\left(E(R)-\frac{\pi Q_{\text{tot}}^2}{L_xL_y}R\right). \tag{9}$$

Notice that Eq. (9) is the result of a formal regularization of the divergent lattice sum (1). We will show in Sec. II B that this formal regularization is equivalent to a neutralization of the system by two charged walls.

Forces follow by differentiation of this potential energy function with respect to particle positions. As the regularizing term in Eq. (9) is independent of particle positions, it does not give rise to any contribution to the forces, as required. Notice that the lattice sum for the force, given by Eq. (1) with an additional gradient operator $-\nabla_i$, is conditionally convergent from the start in systems with a net charge, and hence well defined once the summation order is specified.

B. Interpretation of energies

The regularization (9) of the energy can be interpreted as a neutralization of the system by two charged walls located on each side of the slab, at $z=\pm h/2$, that carry a surface charge density

$$\sigma=-\frac{Q_{\text{tot}}}{2L_xL_y}. \tag{10}$$

These walls can be thought of as arising from a uniform neutralizing charge density created by the particles treated implicitly in the regions above $(z>h/2)$ and below $(z<-h/2)$ the slab. Since these walls exert (constant) equal and opposite forces on charged particles located in between them, they have no net physical effect, apart for a shift in the energy. Let us show that the presence of the two walls regularizes the energy (3) in accordance with the prescription (9) and determine the shift in the energy that results from the particle-wall and wall-wall interactions.

As interactions are summed in a cylindrical limit, we treat the walls as large circular plates of radius $R\to\infty$. The electrostatic potential created by a plate of radius R with surface charge σ reads

$$\Phi_R(z)=\int_0^R\int_0^{2\pi}\frac{\sigma}{\sqrt{r^2+z^2}}r dr d\phi = 2\pi\sigma(\sqrt{R^2+z^2}-|z|) \tag{11}$$

at a distance z from the plate on its symmetry axis. When R is large, $\Phi_R(z)$ behaves as

$$\Phi_R(z)=2\pi\sigma(R-|z|)+\mathcal{O}\left(\frac{1}{R}\right). \tag{12}$$

Two large circular plates at $\pm h/2$ create therefore a constant electrostatic potential in between the plates given by

$$\Phi_{\text{slab}}=2\pi\sigma(2R-h), \quad R\to\infty. \tag{13}$$

The interaction energy of the charges in the simulation box with the two neutralizing walls is therefore

$$E_{c\text{-}w}(R)=Q_{\text{tot}}\Phi_{\text{slab}}=-\frac{\pi Q_{\text{tot}}^2}{L_xL_y}(2R-h). \tag{14}$$

The mutual interaction energy of the walls is (per cell)

$$E_{w_1\text{-}w_2}(R)=\Phi_R(h)\sigma L_xL_y=\frac{\pi Q_{\text{tot}}^2}{2L_xL_y}(R-h), \tag{15}$$

while the self-energies of the two walls read (per cell)

$$E_{w_1\text{-}w_1}(R)+E_{w_2\text{-}w_2}(R)=2\frac{1}{2}\sigma L_xL_y\Phi_R(0)=\frac{\pi Q_{\text{tot}}^2}{2L_xL_y}R. \tag{16}$$

Combining Eqs. (14)–(16) with Eq. (3), the electrostatic energy of the system complemented with the two neutralizing walls is

$$\tilde{E}=\lim_{R\to\infty}\left(E(R)-\frac{\pi Q_{\text{tot}}^2}{L_xL_y}R\right)+\frac{\pi Q_{\text{tot}}^2 h}{2L_xL_y}. \tag{17}$$

The neutralization by two walls gives therefore energies that agree with the regularized energies (9), apart for an

h-dependent term that does not depend on the particle positions. That term is a constant shift in the energy that can be dropped because it has no physical significance.

In summary, the energy of a system carrying a net charge in 2D-PBC is defined by Eq. (9), which can be interpreted as the energy of the system neutralized by two walls, with the prescription that the constant h-dependent shift in the energy is omitted. The present regularization procedure to simulate slab systems with a net charge constitutes the first significant result of this paper.

C. Systems with a changing net charge

The computation of the solvation free energy of ions at infinite dilution is an example where a simulation box with a net charge is used.[17] When computing this free energy via the thermodynamic integration method, the ion is progressively charged, and the charging free energy can be determined from the measured fluctuations of the solute electrostatic energy.[14] Let us show that charging free energies can be correctly computed in 2D periodic systems using definition (9) of the energy, despite the fact that the net charge Q_{tot} varies during the simulation.

As shown in Appendix B, the energy (9) can be written using an effective kernel $\phi_{\mathrm{PBC}}(\boldsymbol{r})$ which takes into account the 2D-PBC:

$$E = \frac{1}{2}\sum_{i,j=1}^{N} q_i q_j \phi_{\mathrm{PBC}}(\boldsymbol{r}_i - \boldsymbol{r}_j). \tag{18}$$

We assume now that a charge q is added at position $\boldsymbol{r}$. The energy of this new system is

$$E_q = E + \frac{1}{2}\left(2\sum_{i=1}^{N} q_i q \phi_{\mathrm{PBC}}(\boldsymbol{r}_i - \boldsymbol{r}) + q^2 \phi_{\mathrm{PBC}}(\boldsymbol{0})\right), \tag{19}$$

where $\phi_{\mathrm{PBC}}(\boldsymbol{0})$ is the regularized interaction energy of a single unit charge with its own periodic images [the value of $\phi_{\mathrm{PBC}}(\boldsymbol{0})$ is computed in Sec. IV A]. One can rewrite Eq. (19) as

$$E_q = E + \int_0^q \Phi_{q'}(\boldsymbol{r}) dq', \tag{20}$$

where

$$\Phi_q(\boldsymbol{r}) = \frac{dE_q}{dq} = \sum_i q_i \phi_{\mathrm{PBC}}(\boldsymbol{r}_i - \boldsymbol{r}) + q\phi_{\mathrm{PBC}}(\boldsymbol{0}). \tag{21}$$

$\Phi_{q'}(\boldsymbol{r})$ is nothing but the electrostatic potential at $\boldsymbol{r}$ created by all other charges in the system and by the periodic images of the charge q' already present at $\boldsymbol{r}$. Equation (20) gives the change in energy when the charge q is added progressively in the system. From Eq. (21), we see that this change in energy is given by the correct expression associated with the 2D-PBC. In particular, the last term in $\Phi_q(\boldsymbol{r})$ gives rise to the charge self-energy $\frac{1}{2}q^2\phi_{\mathrm{PBC}}(\boldsymbol{0})$ which is a known contribution to the energy in PBC.[14,16] The fact that the regularized energy (9) can be written in the form (18) is therefore sufficient to conclude that the energy difference between two systems characterized by a different net charge takes a meaningful value (which includes variations in the self-energies of the charges). Equations (18)–(21) are the counterparts of formally identical formulas that hold in the standard Ewald method for neutral and non-neutral systems in 3D-PBC. As shown in Ref. 14, the charging free energies computed using the Ewald method converge very quickly to their thermodynamical values once a simple correction for finite-size effects is included in the calculations (see also the detailed analysis of finite-size effects of Ref. 18).

The results of this section, together with Eq. (9), show that the thermodynamic integration method can be used to compute charging free energies in inhomogeneous systems with slab geometry. In the present approach, the long-range electrostatic interactions are treated in a manner fully consistent with the 2D periodicity.

III. FAST COMPUTATIONS OF ENERGIES AND FORCES

The regularized energy (9), and the forces on particles derived from it, can be computed quickly in simulations, thanks to advanced algorithms, as detailed in the next sections.

A. MMM2D method

In the MMM2D method,[7] a convergence factor $\exp(-\beta|\boldsymbol{r}_i - \boldsymbol{r}_j + n_x\boldsymbol{L}_x + n_y\boldsymbol{L}_y|)$ is introduced in the energy (1), and the sum is computed in the limit $\beta \to 0$ using an $\mathcal{O}(N^{5/3})$ algorithm.

When the system is non-neutral, the large distance charge-charge interactions generate a divergent contribution as $\beta \to 0$. By the same reasoning as that which leads to Eq. (8), the diverging behavior is given by

$$\frac{1}{2}Q_{\mathrm{tot}}\int_0^\infty \sigma_{\mathrm{sheet}}\frac{\exp(-\beta r)}{r}2\pi r dr = \frac{\pi Q_{\mathrm{tot}}^2}{L_x L_y}\frac{1}{\beta}. \tag{22}$$

The convergence factor approach is thus equivalent to the cylindrical limit approach with the role of variable R played by $1/\beta$. The MMM2D method can therefore be used to compute the regularized energy (9) and forces by simply dropping the divergent contribution (22) in the MMM2D formulae for the energy. As contribution (22) vanishes in a charge neutral system, it is already omitted in the MMM2D method, which can hence be used without any modification to simulate non-neutral slab systems, with energies and forces defined according to Sec. II.

B. The Yeh–Berkowitz approach: EW3DC method

In the EW3DC method of Yeh and Berkowitz,[9] a gap is introduced in the simulation box along the nonperiodic z-direction and a standard Ewald code for 3D-periodic systems is used, typically in a fast $\mathcal{O}(N \log N)$ particle-mesh implementation such as P3M[10] or SPME.[11] The interactions must be summed in a slabwise order. The surface term (also known as the dipole term) in the Ewald formula for the energy takes then the form

$$E^{(d)} = \frac{2\pi}{V} M_z^2, \tag{23}$$

where $M_z = \Sigma_i q_i z_i$ is the total dipole moment of the simulation box along the direction normal to the slab and $V = L_x L_y L_z$ is the volume of the box. The dipole term contributes not only to the energy but also to forces via the expression $\boldsymbol{F}_i^{(d)} = -\boldsymbol{\nabla}_i E^{(d)}$, i.e., it leads to a normal force

$$\boldsymbol{F}_i^{(d)} = -\frac{4\pi M_z}{V} q_i \hat{\boldsymbol{e}}_z \tag{24}$$

on particle i. Since M_z depends on the choice of the origin in systems with a net charge, the EW3DC method obviously cannot be applied to such systems without modification.

When using the Ewald method for a system with a net charge in 3D-PBC, it is assumed implicitly that there are particles distributed uniformly in the simulation box so that they create a constant background charge density $\rho_b = -Q_{\text{tot}}/V$, which neutralizes the system. This neutralization obviously differs from the two walls neutralization defined in Sec. II. Results of the EW3DC approach applied to a system with a net charge will hence need to be corrected [see Eq. (28)] to avoid spurious effects arising from unwanted interactions of the particles with the background charge ρ_b (in particular, the background charge located in region $-L_z/2 \le z \le L_z/2$).

The background charge ρ_b contributes to the Ewald energy not only via Eq. (5) (together with the cancellation of the $\boldsymbol{k}=\boldsymbol{0}$ term in the reciprocal Ewald sum), but also via the dipole term (23), because the background charge has to be accounted for when computing the total dipole moment M_z of the simulation box. Let us fix the origin of our Cartesian coordinate system at the center of the box. The contribution of the background charge to the total dipole moment vanishes then by symmetry, allowing expression (23) to be used without modification.

We assume that the gap in the simulation box is large enough so that interactions between the slab and the unwanted replicas of the slab in the z-direction are entirely negligible (see Sec. IV). The simulated system can then be viewed as a charged slab, of width h, embedded into another slab of width L_z carrying a neutralizing charge density ρ_b. This charge density does not contribute to the dipole term, as with our choice of the coordinate system, its dipole moment is zero. Moreover, the Yeh–Berkowitz approach relies on the fact that for a sufficiently large L_z, the interaction of the charges in the primary slab with the image charges in the z-direction can be approximated by a homogeneous charge distributions. Under this assumption, the interactions with the charges and the background ρ_b in the image slabs cancel, and we are left with the contribution of the background only in the primary slab itself. The electrostatic energy of the system clearly depends on the position of the particles within the larger neutralizing slab, because the latter slab produces a parabolic electrostatic potential

$$V_0(z) = -2\pi\rho_b \int_{-L_z/2}^{L_z/2} |z - z'| dz' = -2\pi\rho_b \left(z^2 + \left(\frac{L_z}{2} \right)^2 \right). \tag{25}$$

The fact that the energy depends on the position of the charged slab system along the z-axis can also be seen on the level of the Ewald formula: The total dipole moment M_z in the surface term (23) clearly depends on the position of the slab in the simulation box. Note that we use here again Eq. (12) but leaving out the R-dependent term, which leads to the divergent contribution (8) already accounted for in the 3D Ewald method with slabwise summation order. To recover the energy of the system defined by the regularization procedure of Sec. II, we only have to subtract the interaction energy of the primary charges with the neutralizing slab, namely,

$$E_{c\text{-}b} = \sum_i q_i V_0(z_i) = -2\pi\rho_b \left(\sum_i q_i z_i^2 + Q_{\text{tot}} \frac{L_z^2}{4} \right), \tag{26}$$

and the self-interaction of the background slab, i.e.,

$$E_{b\text{-}b} = \frac{1}{2} L_x L_y \int_{-L_z/2}^{L_z/2} \rho_b V_0(z) dz = 2\pi\rho_b Q_{\text{tot}} \frac{L_z^2}{6}. \tag{27}$$

We find thus that the contribution

$$E_{\text{bcc}} := -(E_{c\text{-}b} + E_{b\text{-}b}) = 2\pi\rho_b \left(\sum_i q_i z_i^2 + Q_{\text{tot}} \frac{L_z^2}{12} \right), \tag{28}$$

which we call the background charge correction (bcc) term, must be added to the Ewald energies when applying the EW3DC approach to a system with a net charge.

In summary, to simulate a charged slab system using the EW3DC approach, one uses a standard 3D-Ewald code with slabwise summation order, i.e., with surface term (23), in a simulation box with a large enough gap. The interaction energy (5) with the neutralizing background must be included (since the EW3DC approach computes the 3D Ewald energy $E_{\text{3D}} = E^{(r)} + E^{(k)} + E^{(d)} + E^{(n)}$), and the correction term (28) must be added to remove the effect of the parabolic potential created by the neutralizing background slab. Combining Eq. (28) with Eq. (23) yields a corrected surface term given by expression

$$E_{\text{bcc}}^{(d)} := E^{(d)} + E_{\text{bcc}} = \frac{2\pi}{V} \left(M_z^2 - Q_{\text{tot}} \sum_i q_i z_i^2 - Q_{\text{tot}}^2 \frac{L_z^2}{12} \right). \tag{29}$$

Notice that $E_{\text{bcc}}^{(d)}$ is independent of the z-position of the slab in the simulation box, i.e., it is invariant under translations $z \to z + a$ for any value of a, as it should for a system in the $2\text{D}+h$ geometry. There is thus no specific condition on the origin of the coordinate system when using Eq. (29). Forces follow by differentiation of the energy. Taking the negative gradient of Eq. (29) with respect to z_i, one obtains the expression

$$-\nabla_i(E_{\mathrm{bcc}}^{(d)}) = -\frac{4\pi}{V}(M_z - Q_{\mathrm{tot}}z_i)q_i\hat{\boldsymbol{e}}_z \tag{30}$$

for the contribution to the force on the ith particle arising from the surface term and from the bcc. The corrected surface terms (29) and (30) are needed to extend the widely used EW3DC method to non-neutral systems, in accordance with the regularization scheme introduced in Sec. II. This constitutes the second important point of this paper. It is interesting to note that the final result (30) for the force agrees with a new interpretation of the surface term of the Ewald method proposed in Ref. 19. In that reference, the authors derive Eq. (30) from an analysis of the surface term in the 3D-Ewald method for different summation orders (in particular, slabwise), considering also non-neutral systems but without referring to any neutralizing background. We stress, however, that, whatever the summation order, the real-space interaction energy (5) with the neutralizing background charge must be included when computing Ewald energies to avoid results that depend on the free Ewald parameter α.

C. The electrostatic layer correction: P3M/ELC method

The P3M/ELC method[12] uses the same Yeh–Berkowitz approach based on a gap, but it is much more efficient than the EW3DC method because it includes an ELC term that subtracts the interactions of the slab with the unwanted replicas of the slab in the nonperiodic direction. The ELC term allows to reduce significantly the size of the gap needed in the simulation box, and hence the computation effort. Error estimates exist moreover for the ELC term.[12] Since the EW3DC method is a particular case of the P3M/ELC method where the ELC is entirely neglected, the error estimate of the latter method can actually be used to control the accuracy of the EW3DC method as well. As shown by Eq. (18) of Ref. 12, the accuracy of these gap methods is essentially proportional to $\exp(-2\pi Kg)$, where K is the ELC cutoff and g the width of the gap. The EW3DC method does not involve any ELC terms; therefore the cutoff is essentially $K=\min(L_x^{-1},L_y^{-1})$, and consequently the error is controlled by the ratio $g/\max(L_x,L_y)$ and not by the ratio h/L_z as claimed in the original EW3DC paper[9] and still commonly believed.

Not surprisingly, for non-neutral systems, one has to use in P3M/ELC exactly the same bcc (29) as in the EW3DC method. This correction is included in the formula for the ELC term derived recently in the most general case of a (possibly non-neutral) slab system in-between dielectric walls.[20] The algorithm described in Ref. 20 can thus be used without modification[21] to compute energies and forces in charged slab systems, in agreement with the regularization procedure of Sec. II.

IV. NUMERICAL TESTS

In this section the correctness and accuracy of the results stated in Sec. II are tested numerically by computing energies and forces in simple systems, using Eq. (9) with direct summation on one hand and the methods MMM2D, EW3DC, and P3M/ELC on the other hand. To specify what electrostatic method is used in the EW3DC approach, we add a suffix "slab" to the method, which yields denominations such as Ewald/slab, P3M/slab, or SPME/slab for the various incarnations. When the ELC term is employed in these methods to substract the unwanted interlayer interactions, we denote the methods by Ewald/ELC, P3M/ELC, and SPME/ELC.

A. Madelung energy of a 2D square charge lattice

We consider a square simulation box ($L_x=L_y=L$) containing a single charge q under 2D-PBC. The regularized electrostatic energy (9) of this system is equal to the sum of the Coulomb interactions of the charge with all its periodic images and with a neutralizing sheet in the plane of the 2D charge lattice (because the two neutralizing walls coalesce into a single sheet since $h=0$). The energy of this system takes the form

$$E = -\frac{q^2}{2}\phi_{\mathrm{PBC}}(\mathbf{0}) = -\frac{q^2}{2}\frac{\mathcal{F}}{L}, \tag{31}$$

where $\mathcal{F}$ is a dimensionless constant. Using the regularized direct-space sum (9) to compute this Madelung energy, we obtain $\mathcal{F}\simeq 3.9$. A high accuracy is difficult to attain with formula (9) because it expresses the energy as a difference between two large numbers and also because the convergence with R is slow. Nijboer and Ruijgrok found $\mathcal{F}\simeq 3.900\,26$ by using another formula better suited for this purpose.[22]

Using the MMM2D method implemented in the simulation package ESPRESSO (Ref. 23) and tuning the algorithm to accuracy 10^{-10}, we obtain

$$\mathcal{F} \simeq 3.900\,264\,920\,0, \tag{32}$$

where the precision is mainly limited by the employed implementation of the Bessel functions. The MMM2D method clearly works for non-neutral systems and is able to compute quickly 2D Madelung energies to a very high accuracy.

We computed also the energy of this Madelung system by using the P3M/ELC method also implemented in ESPRESSO. We used an accuracy goal of 10^{-4}, which resulted in the following values for the various parameters: Ewald splitting coefficient $\alpha=7.251\,84L^{-1}$, real-space cutoff $r_{\mathrm{cut}}=0.45L$, mesh with 32 points in each direction, charge assignment order=6, gap size=$0.1L$, and ELC far cutoff $=26/L$. This calculation reproduced the first five digits of $\mathcal{F}$, thus validating the bcc (29) for the EW3DC and P3M/ELC methods.

B. Forces between two particles

In molecular dynamics simulations, one is mainly interested in the accuracy of the force computation, since the forces govern the dynamics of the system. Figure 1 shows the pair force between two like charged unit point charges at (0,0,0) and $(1,1,z)$ in a unit cell of dimensions $L_x=L_y=L_z=L=10$ under 2D-PBC; z changes from 0 to L. This system is characterized by a net charge $Q_{\mathrm{tot}}=2$ and a varying dipole

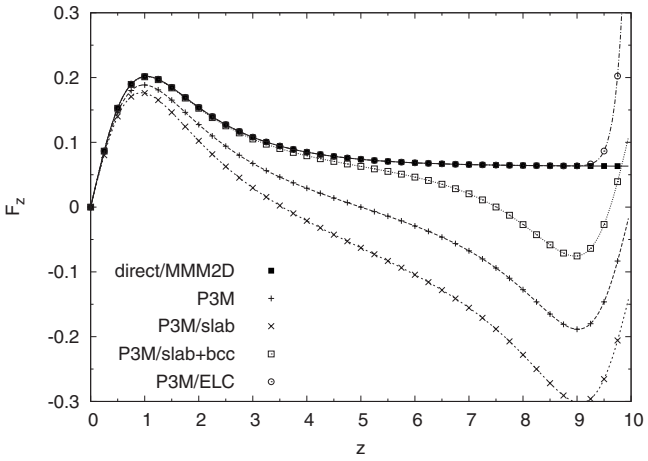

FIG. 1. The force F_z between two unit charges at a relative position of $(1,1,z)$, as a function of z for various algorithms. P3M/slab stands for the EW3DC approach using P3M as the underlying electrostatic method, while P3M/slab+bcc is the same method with the addition of the bcc (30).

moment $M_z=qz$; therefore it is well suited to demonstrate the effect of the net charge in the various electrostatic methods that we tested:

- Well-converged direct summation taking into account 100^2 images,
- MMM2D method of Ref. 7,
- P3M with metallic boundary conditions, i.e., without surface term,
- P3M with the slab-corrected surface term following Ref. 9,
- P3M with the slab-corrected surface term and bcc (30),
- P3M with the ELC extension following Ref. 20.

MMM2D and the direct summation agree in at least two digits; therefore only the results for MMM2D are shown. MMM2D was again tuned for a precision of at least 10^{-10}, and P3M and ELC for a precision better than 10^{-4}. When $z > L/2$, the force computed with direct summation and MMM2D takes its asymptotic value $2\pi/(L_xL_y)$, which corresponds to the force exerted on a unit charge by a charged sheet with surface charge density $1/(L_xL_y)$.

P3M with slabwise summation order and bcc (30) agrees well with the direct summation in the expected range of validity, namely, for $z < L/3$. Correspondingly, P3M with the ELC extension, which was tuned to agree with high precision for $z < L_z/2$, agrees well up to $z=9$. In contrast to this, applying only the slab correction of Ref. 9 actually *increases* the error of the plain P3M method with metallic boundary conditions.

Would the two unit charges be oppositely charged and hence the system neutral, the force between the charges would simply be the opposite of those presented in Fig. 1. This is indeed the case for all methods, again with the exception of P3M/slab, which gives correct forces only in systems with no net charge.

V. EXAMPLE: MEAN FORCE ON AN ION NEAR AN INTERFACE

A precise understanding of the adsorption, or depletion, of ions near an interface is important in several fields, for example, in biophysics, where the hydrophobic solid/water interface governs the aggregation and folding of apolar molecules, and in atmospheric chemistry, where physicochemical processes occur at the air/water and ice/water interfaces. Potentials of mean force for ions at infinite dilution have been obtained recently at such interfaces.[24–26] In these works, the simulated systems had a net charge and the long-range nature of the Coulomb force was taken into account by using 3D Ewald summations with a gap in the simulation box (EW3DC method if the summation order was changed to slabwise). As shown in Sec. IV, it is essential to include the newly derived bcc (30) for the electrostatic forces to be correct in such non-neutral simulations.

According to macroscopic electrostatics, an ion close to a dielectric interface sees an electrostatic potential that corresponds to a (fictitious) image charge located symmetrically on the opposite side of the interface.[27] In the case of an ion close to an air/water interface, the dielectric contrast is about 80, and this image-charge effect is expected to contribute to the mean force on the ion as it approaches the surface. We performed a molecular dynamics simulation of this non-neutral system to show that the EW3DC method, when complemented with the bcc (30), does lead to results that agree with the prediction of macroscopic electrostatics.

The simulation box was setup similarly as in Refs. 24 and 26: A sodium ion carrying charge $q=+e$ is at a distance z from the surface of a water slab of width $h=2.483$ nm made up of 2048 water molecules. The dimensions of the simulation box are $L_x=L_y=2h$ and $L_z=5h$, i.e., a gap of width $4h$ is introduced in the nonperiodic direction normal to the slab. Water molecules are described according to the SPC/E model[28] and the Lennard-Jones parameters for the sodium-water interaction are taken from Ref. 29 in their nonpolarizable form. The simulations were performed using a modified version of the GROMACS simulation package,[30] in which we implemented the bcc. The equations of motion were integrated using the leap-frog algorithm with a time step of 2 ps, and the temperature was kept constant at 300 K using the Berendsen method. The Coulomb interactions were computed using the SPME method[11] with a slabwise summation order and bcc (SPME/slab+bcc). The cutoff for the van der Waals and real-space Coulomb forces are both set to 1 nm.

The sodium ion is free to move in the x-y directions, but its distance to the water surface is kept fixed during each simulation (a rigid constraint prevents the z coordinate of the ion to change). The position of the surface is defined by the criterion that the density of water at the surface is half that of the bulk. For each considered distance of the ion, we performed a 5 ns long simulation to determine the mean force F_z acting on the ion. We simulated also the case of a water surface confined by a (hydrophobic) hard wall located 0.1 nm above the water surface. In the latter case, the water

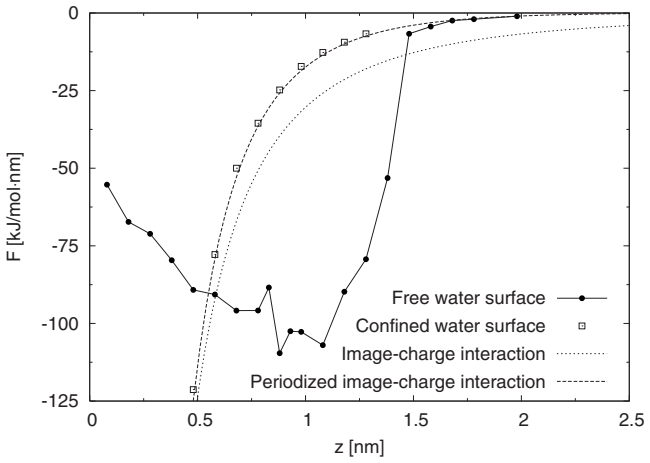

FIG. 2. Mean force on a sodium ion at a distance z from a water surface, which is either free (black circles) or confined by a hydrophobic hard wall located 0.1 nm above the surface (white squares). The image-charge force predicted by macroscopic electrostatics for a dielectric interface located at $z=-0.22$ Å is shown for two different choices of boundary conditions: zero field at infinity (dotted line) and 2D-PBC (dashed line).

molecules whose oxygen atom hit the hard wall were reflected back into the liquid by inverting the z-component of their velocity.

When the water molecules are prevented by the hard wall to partially solvate the ion, the measured force on the ion is well predicted by the image-charge interaction of macroscopic electrostatics (see Fig. 2). According to this theory, an ion of charge q in a medium of permittivity $\epsilon_1 \simeq 1$ (air) and at a distance z from a slab of width h and permittivity $\epsilon_2 \simeq 80$ (water) sees an electrostatic potential[31]

$$\Phi(z) = \frac{q}{\epsilon_1}\left\{ \frac{\epsilon_1-\epsilon_2}{\epsilon_1+\epsilon_2}\frac{1}{2z} - \frac{4\epsilon_1\epsilon_2}{(\epsilon_1+\epsilon_2)^2}\sum_{n=1}^{\infty}\left(\frac{\epsilon_1-\epsilon_2}{\epsilon_1+\epsilon_2}\right)^{2n-1}\frac{1}{2z+2nh}\right\}. \quad (33)$$

The first term in (33) is an image-charge due to the first interface, while the infinite sum corresponds to additional image charges that are due to the presence of the second interface at the other side of the water film. The force on the ion derives from its electrostatic potential energy $\int_0^q \Phi(z)dq = \frac{1}{2}q\Phi(z)$ and is plotted as a dotted line in Fig. 2. The potential (33) corresponds to the interaction of an ion with a dielectric slab under the boundary condition of zero field at infinity, while the electrostatic potential is computed in the simulations under 2D-PBC. To account for this periodicity in the x-y directions, one has to sum up over the periodic images of the image charges. This was done by setting up a cell containing the ion and the infinite set of image charges[32] that appear in Eq. (33) and by computing the force on the ion using the MMM2D method. The result, assuming the continuous dielectric interface to be placed at a distance $d'=0.22$ Å below the molecular water surface, is shown as a dashed line in Fig. 2. That prediction of macroscopic electrostatics agrees very well with the simulation results. The agreement holds at all distances in the case of the confined water surface, while it holds only at large distances in the case of the free water surface. The simulations show that the ion is indeed partially solvated even when quite far away from the water surface (up to $z \simeq 1.45$ nm).

The fact that the dielectric interface is located very close to the molecular water surface agrees with the very sharp dielectric permittivity profile of a water slab determined in Ref. 33. A more detailed analysis of the relative position between the molecular water surface and the position of the dielectric interface (in the case of a confinement more realistic than a hard wall) will be performed in a future work.

We note that finite-size effects are quite pronounced with the size of the simulation box used in this example. The prediction of macroscopic electrostatics changes indeed substantially once the periodicity in the x-y directions is introduced (compare dotted and dashed lines in Fig. 2). This is not unexpected since Coulomb interactions with image charges in the neighboring cells are negligible only if L_x and L_y are sufficiently large. To determine a force profile that is free from finite-size effects, a larger simulation box should clearly be used.

Because of the use of the slab geometry, the ion sees two dielectric interfaces instead of a single one. This unwanted feature can be avoided by introducing a hard wall with the same dielectric permittivity as water at the other side of the slab. This will remove almost entirely the unwanted effects of the second dielectric interface. The latest versions of the MMM2D and P3M/ELC methods that include image charges can be used to simulate such a slab system with different continuous dielectric media of permittivities ϵ_1 and ϵ_2 at the two sides of the slab.[20,34]

VI. CONCLUSIONS

A regularization of the electrostatic energy of 2D periodic slab systems bearing a net charge has been proposed. That regularization is the analog in 2D-PBC of the usual regularization of Ewald sums in three dimensions by a homogeneous neutralizing background charge density. The regularized energies, given by Eq. (9), can be interpreted as resulting from a neutralization of the system by two charged walls on each side of the slab, with the prescription that the constant shift in the energy proportional to the wall-wall separation is omitted. We proved that energy differences between two systems characterized by a different net charge take meaningful values, which include variations in the self-energies of the charges in 2D-PBC. The method can thus be used to simulate systems with a varying net charge, for example, to determine charging free energies in inhomogeneous systems with slab geometry.

The regularized energies, and the forces that derive from them, can be computed efficiently by using advanced electrostatic algorithms for 2D periodic systems, such as MMM2D, EW3DC, and P3M/ELC. We proved that the MMM2D method can be applied without any modification to non-neutral systems, while methods based on the EW3DC approach necessitate the use of a bcc, given by Eq. (28), which affects both energies and forces. The bcc removes the

effect of the parabolic electrostatic potential inherited from the neutralization of the cell implicit in the 3D-Ewald method applied to a charged slab system.

Numerical tests have been done to demonstrate the correctness and the accuracy of the results. When the bcc is added to the EW3DC results, the three methods (MMM2D, EW3DC+bcc, and P3M/ELC) give consistent results for the energies and forces, that agree also with well converged direct-sum calculations. As shown in Fig. 1, the application to non-neutral systems of the uncorrected EW3DC approach leads to incorrect forces which are even further away from the reference direct-sum result than the plain 3D-Ewald method with metallic boundary conditions. We stress that the surface terms with bccs (29) and (30) are easy to evaluate and have no computational cost in a simulation.

The three methods reproduce the known value of the Madelung self-energy on an ion in 2D-PBC, which can be computed quickly to very high accuracy using the MMM2D method. That energy, given by $E_{\text{self}}=-q^2\mathcal{F}/(2L)$ with $\mathcal{F}\simeq 3.900\,264\,920\,0$ in a square simulation box ($L_x=L_y=L$), plays an important role in the stability of 2D Wigner crystals, in charging free energy calculations under PBC and in the study of finite-size effects.[18,22,35]

A further demonstration that our method provides correct long-range electrostatic forces is provided in the form of a calculation via molecular dynamics simulations of the mean force on a sodium ion close to an air/water interface. A nice agreement with the image-charge prediction of macroscopic electrostatics is observed within the limits of validity of the theory. The dielectric discontinuity at the air/water interface in the macroscopic model is found to be situated at the very surface of the water slab (at a distance of 0.22 Å under the molecular water surface defined by the criterion used in Sec. V).

We expect the results of the present work to be of wide applicability to simulations of slab systems whenever an implicit uniform background of charges can be assumed. Research works related to the calculation of ionic solvation free energies, study of surfaces with charged defects, bilayers of charged particles, etc., can substantially benefit from the derivations made in the present study.

ACKNOWLEDGMENTS

J. J. Cerdà wants to thank the financial support of the Spanish Ministerio de Educación *y* Ciencia, postdoctoral Grant No. EXP2006-0931. All authors are grateful to the DAAD organization and the French *Ministère des affaires étrangères et européennes* for providing financial support.

APPENDIX A: ENERGY DENSITY AND FACTORS 1/2

This appendix explains the origin of factor 1/2 in some formulas, for example Eq. (1) when $(n_x,n_y)\neq(0,0)$ and Eqs. (7) and (8), but not in others such as Eqs. (6) and (14). We first note that, as a rule of thumb, interaction energy $E_{a\text{-}b}$ between two identical objects ($a=b$) gets a factor 1/2, while no such factor must be included when $a\neq b$.

The factor 1/2 is a consequence of the fact that, when using PBC, the energy that one computes is not the total energy of the simulation box itself, but the energy *per box* of the macroscopic sample made up of many copies of the primary cell. Indeed, dividing the macroscopic sample in B boxes, its energy can be written as

$$E_{\text{sample}}=\sum_{b=1}^{B}E_b+\frac{1}{2}\sum_{\substack{b,b'=1\\ b'\neq b}}^{B}E_{b\text{-}b'}, \tag{A1}$$

where E_b is the energy of box b and $E_{b\text{-}b'}$ is the interaction energy between particles in box b and particles in box b'. Since the macroscopic sample is large, the number of boxes near the surface of the sample is negligible in front of the number of boxes in the volume of the sample. We can therefore write, assuming a homogeneous sample divided in B identical boxes of volume V_b,

$$\frac{1}{2}\sum_{\substack{b,b'=1\\ b'\neq b}}^{B}E_{b\text{-}b'}\simeq B\frac{1}{2}\sum_{\substack{b'=1\\ b'\neq\text{primary box }b}}^{B}E_{b\text{-}b'}. \tag{A2}$$

We conclude that the energy per box is

$$E:=\frac{E_{\text{sample}}}{B}=E_b+\frac{1}{2}\sum_{\substack{b'=1\\ b'\neq\text{primary box }b}}^{B}E_{b\text{-}b'}. \tag{A3}$$

All interactions between the simulation box and the periodic images of the simulation box must therefore be accounted for with a factor 1/2 to avoid double counting in the energy of the macroscopic sample. Notice that the ratio of the energy per box divided by the volume of the simulation box, $e:=E/V_b=E_{\text{sample}}/(V_bB)$, does measure correctly the energy density of the macroscopic sample since V_bB is the volume of that sample. This explains the factor 1/2 in Eq. (1) when $(n_x,n_y)\neq(0,0)$.

When the system contains a neutralizing background, the interaction of the primary box b_1 with an image box b_2 is the sum of four interactions energies (which must all be accounted for with a factor 1/2) between four different entities:

$$E_{b_1\text{-}b_2}=E_{c_1\text{-}c_2}+E_{c_1\text{-}\rho_2}+E_{\rho_1\text{-}c_2}+E_{\rho_1\text{-}\rho_2}, \tag{A4}$$

where c_i (ρ_i) stands for the charges (neutralizing background charge density) in box b_i, $i=1,2$. The absence of factor 1/2 in Eq. (6) results therefore from the fact that this energy is actually the sum of the two energies $E_{c_1\text{-}\rho_2}$ and $E_{\rho_1\text{-}c_2}$ which lead to the same value after summation over all boxes. The energies $E_{c_1\text{-}c_2}$ and $E_{\rho_1\text{-}\rho_2}$ appear only once in Eq. (A4), so there is indeed a factor 1/2 in equations such as Eq. (8) or Eq. (7) when $\boldsymbol{r}'\notin V_{b_1}$. When $\boldsymbol{r}'\in V_{b_1}$, the factor 1/2 in Eq. (7) simply prevents double counting within the box, according to the usual relation

$$\sum_i\sum_{j>i}E_{i-j}=\frac{1}{2}\sum_{\substack{i,j\\ i\neq j}}E_{i-j}. \tag{A5}$$

APPENDIX B: EFFECTIVE KERNEL FORMULATION

In this appendix, we demonstrate that the energy given by Eq. (9) of a charged system under 2D-PBC can be written as a sum over an effective kernel $\phi_{\mathrm{PBC}}(\boldsymbol{r})$ as in (18), similar to the Ewald sum in 3D-PBC.[36,37] To this aim, we reformulate Eq. (3) as

$$E(R) = \frac{1}{2}\sum_{i,j=1}^{N} q_i q_j V(\boldsymbol{r}_i - \boldsymbol{r}_j) + \frac{1}{2}\sum_{i,j=1}^{N} q_i q_j \sum_{(n_x,n_y)\in D(R)} \times \frac{1}{|n_x\boldsymbol{L}_x + n_y\boldsymbol{L}_y|} + \frac{1}{2}\sum_{i,j=1}^{N} q_i q_j \sum_{(n_x,n_y)\in D(R)} \times \left(\frac{1}{|\boldsymbol{r}_i - \boldsymbol{r}_j + n_x\boldsymbol{L}_x + n_y\boldsymbol{L}_y|} - \frac{1}{|n_x\boldsymbol{L}_x + n_y\boldsymbol{L}_y|} \right), \tag{B1}$$

where

$$V(\boldsymbol{r}) = \begin{cases} 0 & \text{if } \boldsymbol{r} = \boldsymbol{0} \\ 1/|\boldsymbol{r}| & \text{if } \boldsymbol{r} \neq \boldsymbol{0}, \end{cases} \tag{B2}$$

and $D(R)$ denotes all $(n_x,n_y)\in\mathbb{Z}^2$ with $0<(n_xL_x)^2+(n_yL_y)^2 \leq R^2$. The first term is already of the desired form; by approximation of the sum by an integral, one can see that the second term is of the form

$$\frac{1}{2}\sum_{(n_x,n_y)\in D(R)} \frac{1}{|n_x\boldsymbol{L}_x + n_y\boldsymbol{L}_y|} = \frac{\pi R}{L_x L_y} + S + \mathcal{O}(R^{-1}), \tag{B3}$$

where the first term added up over all particles gives the singularity $(\pi Q_{\mathrm{tot}}^2/L_xL_y)R$ that is subtracted in Eq. (9), and the constant term S is the self-energy of a unit charge, which is given by $S=-\mathcal{F}/(2L)$ with $\mathcal{F}\simeq 3.900\,26$ in the case of a square lattice $L_x=L_y=L$ [see Eq. (31)]. Regarding the third term in Eq. (B1), we note that for two vectors $\boldsymbol{r}$ and $\boldsymbol{a}$,

$$\frac{1}{|\boldsymbol{r}+\boldsymbol{a}|} + \frac{1}{|\boldsymbol{r}-\boldsymbol{a}|} - \frac{2}{|\boldsymbol{a}|} = \mathcal{O}(|\boldsymbol{a}|^{-3}), \tag{B4}$$

which means that the last sum over (n_x,n_y) in the third term is in fact absolutely convergent provided the summands for (n_x,n_y) and $(-n_x,-n_y)$ are added in pairs, i.e., as in Eq. (B4) with $\boldsymbol{a}=n_x\boldsymbol{L}_x+n_y\boldsymbol{L}_y$ (note that in 3D-PBC, the analogous sum would be only conditionally convergent). Therefore, Eq. (B1) can be written as

$$\lim_{R\to\infty}\left(E(R) - \frac{\pi Q_{\mathrm{tot}}^2}{L_x L_y} R \right) = \frac{1}{2}\sum_{i,j=1}^{N} q_i q_j \phi_{\mathrm{PBC}}(\boldsymbol{r}_i - \boldsymbol{r}_j), \tag{B5}$$

where

$$\phi_{\mathrm{PBC}}(\boldsymbol{r}) := V(\boldsymbol{r}) + S + \lim_{R\to\infty} \sum_{(n_x,n_y)\in D(R)} \times \frac{1}{2}\left(\frac{1}{|\boldsymbol{r} + n_x\boldsymbol{L}_x + n_y\boldsymbol{L}_y|} - \frac{1}{|n_x\boldsymbol{L}_x + n_y\boldsymbol{L}_y|} \right). \tag{B6}$$

[1] D. E. Parry, Surf. Sci. **49**, 433 (1975).
[2] D. M. Heyes, M. Barber, and J. H. R. Clarke, J. Chem. Soc., Faraday Trans. 2 **73**, 1485 (1977).
[3] J. Hautman and M. L. Klein, Mol. Phys. **75**, 379 (1992).
[4] B. R. A. Nijboer and F. W. de Wette, Physica (Amsterdam) **23**, 309 (1957).
[5] E. R. Smith, Mol. Phys. **65**, 1089 (1988).
[6] M. Kawata, M. Mikami, and U. Nagashima, J. Chem. Phys. **116**, 3430 (2002).
[7] A. Arnold and C. Holm, Comput. Phys. Commun. **148**, 327 (2002).
[8] S. Tyagi, Phys. Rev. E **70**, 066703 (2004).
[9] I.-C. Yeh and M. L. Berkowitz, J. Chem. Phys. **111**, 3155 (1999).
[10] R. W. Hockney and J. W. Eastwood, *Computer Simulation Using Particles* (IOP, Bristol, 1988).
[11] U. Essmann, L. Perera, M. L. Berkowitz, T. Darden, H. Lee, and L. G. Pedersen, J. Chem. Phys. **103**, 8577 (1995).
[12] A. Arnold, J. de Joannis, and C. Holm, J. Chem. Phys. **117**, 2496 (2002).
[13] S. Alireza Ghasemi, A. Neelov, and S. Goedecker, J. Chem. Phys. **127**, 224102 (2007).
[14] G. Hummer, L. R. Pratt, and A. E. Garcia, J. Phys. Chem. **100**, 1206 (1996).
[15] A. Arnold and C. Holm, Adv. Polym. Sci. **185**, 59 (2005).
[16] V. Ballenegger, J. J. Cerda, O. Lenz, and C. Holm, J. Chem. Phys. **128**, 034109 (2008).
[17] G. Hummer, L. R. Pratt, and A. E. Garcia, J. Phys. Chem. **102**, 7885 (1998).
[18] P. H. Hünenberger and J. A. McCammon, J. Chem. Phys. **110**, 1856 (1999).
[19] H. D. Herce, A. E. Garcia, and T. Darden, J. Chem. Phys. **126**, 124106 (2007).
[20] S. Tyagi, A. Arnold, and C. Holm, J. Chem. Phys. **129**, 204102 (2008).
[21] Note that the last term in Eq. (3.10) of Ref. 20 should have a minus sign.
[22] B. R. A. Nijboer and Th. W. Ruijgrok, J. Stat. Phys. **53**, 361 (1988).
[23] H. J. Limbach, A. Arnold, B. A. Mann, and C. Holm, Comput. Phys. Commun. **174**, 704 (2006) (http://espresso.mpg.de).
[24] P. Jungwirth and D. J. Tobias, Chem. Rev. (Washington, D.C.) **106**, 1259 (2006).
[25] E. J. Smith, T. Bryk, and A. D. J. Haymet, J. Chem. Phys. **123**, 034706 (2005).
[26] D. Horinek and R. R. Netz, Phys. Rev. Lett. **99**, 226104 (2007).
[27] J. D. Jackson, *Classical Electrodynamics*, 3rd ed. (Wiley, New York, 1999).
[28] H. J. C. Berendsen, J. R. Grigera, and T. P. Straatsma, J. Phys. Chem. **91**, 6269 (1987).
[29] D. E. Smith and L. X. Dang, J. Chem. Phys. **100**, 3757 (1994).
[30] E. Lindahl, B. Hess, and D. van der Spoel, J. Mol. Model. **7**, 306 (2001) http://www.gromacs.org.
[31] G. Iversen, Y. I. Kharkats, and J. Ulstrup, Mol. Phys. **94**, 297 (1998).
[32] It is actually sufficient to introduce only the two first image charges: a charge $q_1=-q(\epsilon_1-\epsilon_2)/(\epsilon_1+\epsilon_2)$ at position $-z$ and a charge $q_2=-q_1$ at position $-(z+h)$. Notice that $q_1+q_2=0$ in accordance with the charge neutrality of the slab.
[33] V. Ballenegger and J.-P. Hansen, J. Chem. Phys. **122**, 114711 (2005).
[34] S. Tyagi, A. Arnold, and C. Holm, J. Chem. Phys. **127**, 154723 (2007).
[35] S. Bogusz, T. E. Cheatham III, and B. R. Brooks, J. Chem. Phys. **108**, 7070 (1998).
[36] S. W. de Leeuw, J. W. Perram, and E. R. Smith, Proc. R. Soc. London, Ser. A **373**, 27 (1980).
[37] G. Hummer, L. R. Pratt, and A. E. Garcia, J. Phys. Chem. **99**, 14188 (1995).